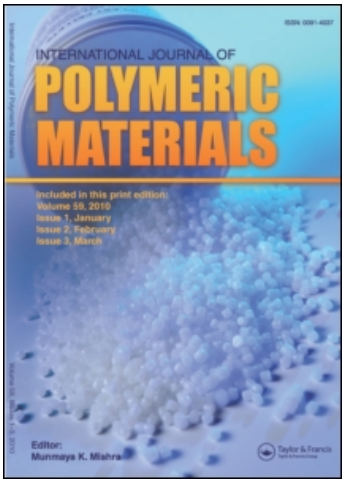

International Journal of Polymeric Materials
Publication details, including instructions for authors and subscription information:
http://www.informaworld.com/smpp/title~content=t713647664

Polymer Composites with Electrophysical Properties

A. T. Ponomarenko[a]; V. G. Shevchenko[a]; Yu. G. Kryazhev[b]; V. N. Kestelman[c]
[a] Institute of Synthetic Polymeric Materials, Russian Academy of Sciences, Moscow, Russia [b] Institute of Carbon Materials, Kemerovo, Russia [c] JBK International, Pennsylvania, USA

To cite this Article Ponomarenko, A. T. , Shevchenko, V. G. , Kryazhev, Yu. G. and Kestelman, V. N.(1994) 'Polymer Composites with Electrophysical Properties', International Journal of Polymeric Materials, 25: 3, 201 — 226
To link to this Article: DOI: 10.1080/00914039408029338
URL: http://dx.doi.org/10.1080/00914039408029338

Intern. J. Polymeric Mater., 1994, Vol. 25, pp. 201–226
Reprints available directly from the publisher
Photocopying permitted by license only

Printed in Malaysia

Polymer Composites with Electrophysical Properties

A. T. PONOMARENKO, V. G. SHEVCHENKO, YU. G. KRYAZHEV,*
V. N. KESTELMAN†

Institute of Synthetic Polymeric Materials, Russian Academy of Sciences, Moscow, Russia
**Institute of Carbon Materials, Kemerovo, Russia*
†*JBK International, Pennsylvania, USA*

(Received October 5, 1993)

Electrophysical properties of polymer composites with disperse, fiber or fabric fillers are examined. The methods for controlling their electrical, magnetic, thermal and other properties by changing the ingredients and compounding methods are reported. Some examples of using polymer composites in the form of functional elements or structures, prospective for different fields of science and technology are presented.

KEY WORDS Polymer composites, electrical properties

1. INTRODUCTION

New polymer composites are now being intensely developed, whose functional characteristic property is the transport of charge carriers in *dc* and *ac* electromagnetic fields, while at the same time they have a definite level of electrical and heat conductivity, magnetoresistance or real and imaginary parts of dielectric and magnetic permittivities.[1] Progress in this important field is possible on the basis of detailed electrophysical investigations and taking into account multiple factors, such as composition of the material, method of compounding the ingredients, preparation of laboratory samples, structures and articles.

Figure 1 shows filler shapes and their possible packings in polymer matrix. Present work treats mostly electrophysical properties of composite materials (CM) with disperse (metal or carbon) in the form of spheres, cubes, flakes or fibers, and carbon fibrous (short, continuous) or fabric fillers.

We, the beginners in the field of CM 15 years ago, were greatly impressed by an article, that clearly demonstrated the influence of processing technology on percolation thresholds (Reference 2, Figure 2). Later (Figure 3) the dependence of conductivity on the type of filler was clearly demonstrated.[3] We think that these works had a great impact on investigations in this field and stimulated its progress.

Characteristic features of the present investigations was the use of advanced

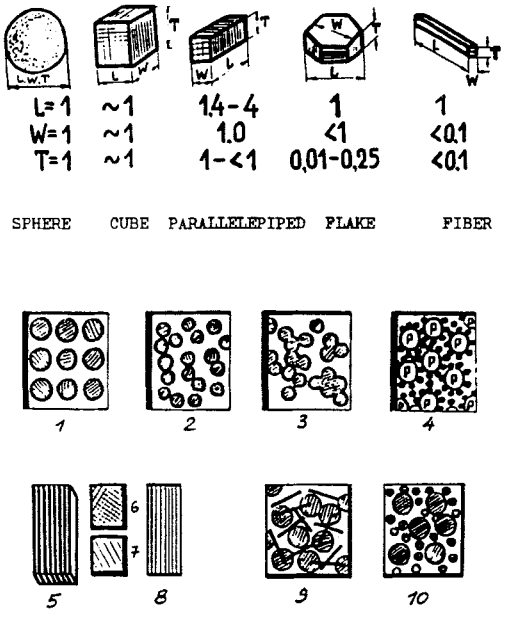

FIGURE 1 Distribution of fillers in polymeric matrix: (1) matrix system; (2) statistical distribution; (3 and 4) structured composites; (5) conducting fabric composite; (6, 7 and 8) conducting fiber composite; (9) short fiber and particle composite; and (10) composite with particles of different size.

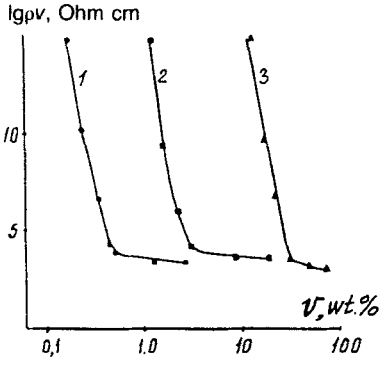

FIGURE 2 Dependence of ρ, of polystyrene composites on Ketjenblack EC carbon black concentration v, prepared by different methods: (1) mechanical mixing of powders, pressure molding; (2) mixing in a ball mill of toluene solution of PS with carbon black, evaporation of toluene, casting of film, grinding, pressure molding; and (3) calendering, grinding, pressure molding. (Clason, Kubat, 1975).

physical methods in order to understand in what direction it is possible to regulate electrophysical properties of polymeric CM and find the ways to increasing coefficients of realization of their components. From the examples quoted in the paper it follows that the aim is achieved through the use of advanced technologies, optimized compositions and methods for the formation of structures from polymeric composites, adequate to their electrophysical properties and functional possibilities.

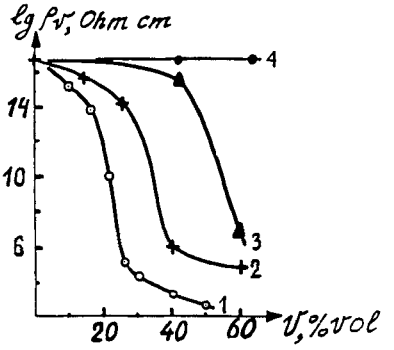

FIGURE 3 Dependence of resistivity ρ_v of LDPE composites on conducting filler concentration: (1) acetylene black; (2) graphite ZKA; (3) aluminum powder PAK-3; and (4) zinc dust.

2. ELECTROPHYSICAL PROPERTIES OF DISPERSE PARTICLES FILLED COMPOSITES

Disperse particles filled composites were produced by the methods of polymerization on filler surface[4-6] and modified mechanical mixing of ingredients, such as melt mixing, "cold" extrusion and "dry" mixing.[7]

2.1. Properties of Metal Particles Filled Composites in *DC* Electric Field

Several types of polymer composites were investigated, among them Al-[8-9] and Mo-containing plastics, the method of preparation being as follows.

Alumoplastics—CM, containing spherical Al particles with mean diameter d = 10 μm and oxide film thickness ≈300 Å (oxide content up to 3%). On the surface of particles a metallocomplex catalyst of Ziegler-Natta type was deposited and then propylene polymerization carried out (PFC method). For comparison, mechanical mixtures of Al and polypropylene powders were pressure molded at T = 175 ± 5°C and P = 10 MPa.

Mo-containing composites were prepared by mechanical mixing of Mo powder with mean diameter ≈1 μm and polytetrafluoroethylene (PTFE, d = 10.5 μm), copolymer of styrene and α-methylstyrene (SAM, d = 1.4 μm), or polyvinylbutyral (PVB, d = 6.6 μm) powders. Samples were pressure molded at T = 130°C, P = 10 MPa (PTFE); T = 150°C, P = 65 MPa (SAM); T = 130°C, P = 65 MPa (PVB). Total oxide content in Mo powder was 3–5% wt. with corresponding thickness of the layer on particles 100–160 Å. To evaluate the effect of oxide layer, Mo powder was reduced in hydrogen atmosphere at 1000°C for 2–4 hours.

Figure 4 presents dependences of $\lg\sigma_\perp$ on volume fraction of Al (v in all cases is the filler volume fraction). Percolation threshold for mechanical mixtures is v^* = 0.15, and for polymerization filled CM v^* = 0.45. A rather unique feature of these CM, prepared by PFC method is that $\sigma_\perp = \sigma_\parallel$) if the samples are in the form of cubes. For plates, larger values of σ in direction perpendicular to the molding plane ($\sigma_\perp$) compared to that in the molding plane ($\sigma_\parallel$), i.e. $\sigma_\perp > \sigma_\parallel$, are observed at certain forming field strength $E_\perp^*$ (V/cm) when partial breakdowns occur in the

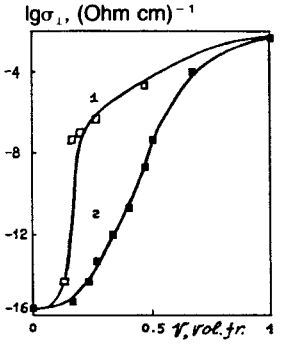

FIGURE 4a Dependence of alumoplastics conductivity on filler volume fraction (*dc*, forming field E = 100 V/cm). (1) mixing of PP and Al powders; (2) PFC method.

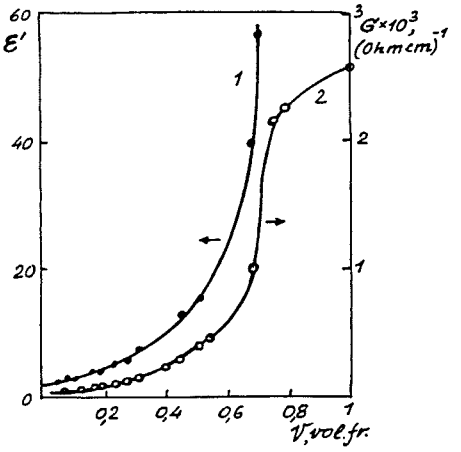

FIGURE 4b Electrodynamic properties of alumoplastics versus Al volume fraction (f = 4.7 GHz). (1) ε' and (2) σ.

sample, making $\sigma_\perp >> \sigma_\parallel$. The value of $\sigma_\perp$ sharply increases after that around v^* = 0.45 (see Figure 1; the measurements were taken at $E^*_\perp$ = 100 V/cm), while $\sigma_\parallel$ in the interval v = 0.06–0.72 remains on the level of 10^{-16} (Ohm·cm)$^{-1}$. From this data it follows that in the interval v = 0.2–0.7 the ratio $\sigma_\parallel/\sigma_\perp = 10^{-2} \div 10^{-12}$ with percolation threshold in $\sigma_\parallel$ being $v > 0.72$.

Electrical properties of Mo-containing composites, prepared by mixing of polymer and filler powders are significantly different from those of alumoplastics (Figure 5). Comparison of conductivity-concentration curves for different polymer matrices gives v^* = 0.07 for PTFE, v^* = 0.17 for SAM and v^* = 0.22 for PVB. It is interesting that for CM with PTFE the value of percolation threshold v^* = 0.07, which is much lower than the theoretical value. Microstructural analysis shows that Mo particles in PTFE form clusters with average size $\bar{n}$ = 8.7 and volume fraction 80–90%, while in PVB the fraction of clusters is much lower – 60% and $\bar{n}$ = 3.5. Very important is the ratio R_p/R_m (R_p and R_m are radiuses of polymer and filler particles, respectively), the increase of which correlates with decrease of v^*.[10] Compared to alumoplastics, Mo CM have high values of $\sigma_\parallel$. For example, at

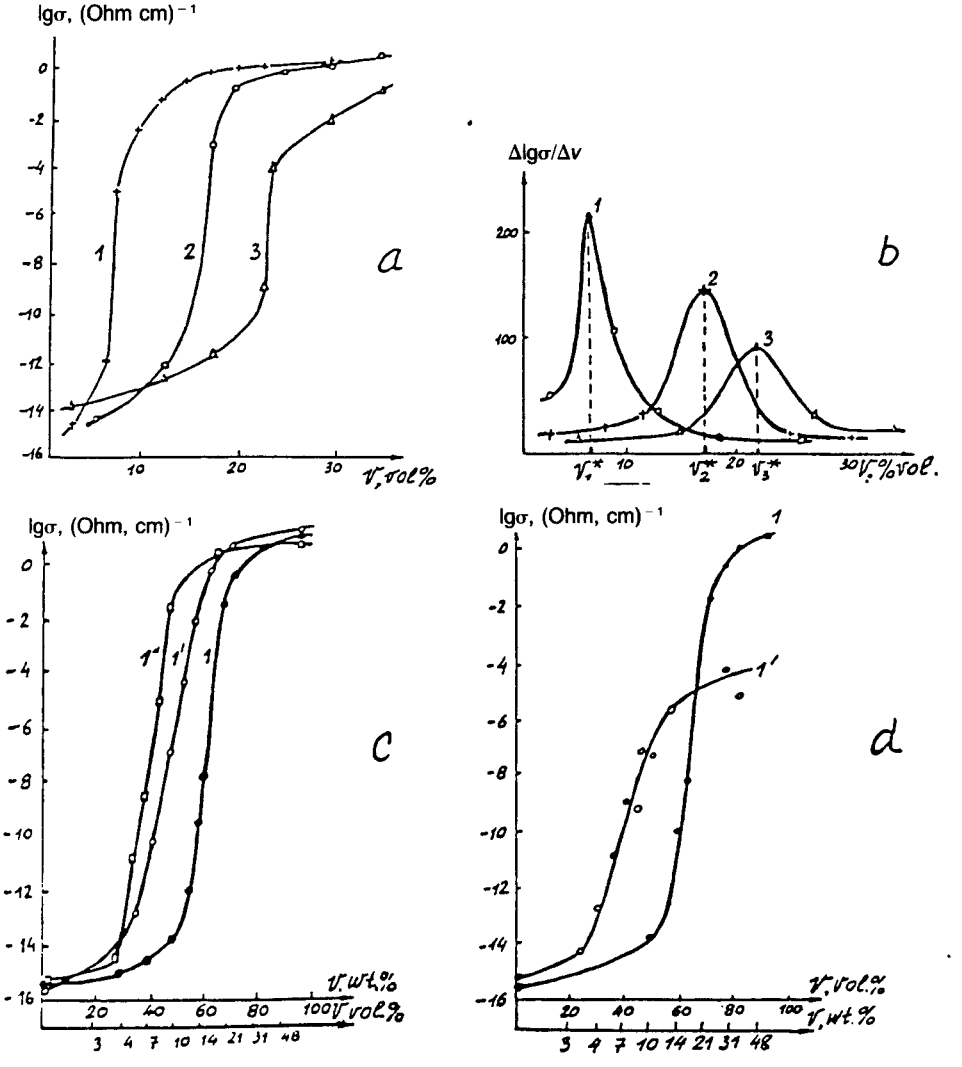

FIGURE 5 Dependence of composite conductivity on Mo powder concentration. a and b: (1) PTFE; (2) copolymer of styrene and α-methylstyrene (SAM); (3) polyvinylbutyral. b: differential curves, v_i^* = percolation thresholds. c: reduction of Mo powder prior to compounding with SAMS: 1 = 0 hours; 1′ = 1000°C, 2 hours; 1″ = 1000°C, 4 hours. d: Mo powders with different particle size: 1 = 1.3 μm; 2 = 0.1 μm.

v = 0.3 for all matrices σ ≃ 1 (Ohm·cm)$^{-1}$. Reduction of oxide layers on Mo particles lowers v^* to 0.04 in 2 hours and v^* = 0.03 in 4 hours (1000°C) for SAM matrix. At the same time, maximum values of σ at v = 0.3 remain practically the same, evidencing high contact resistance between the particles and increasing polymer-filler interaction in the order PTFE-SAM-PVB, leading to the increase of percolation threshold and broadening of the transition to conducting state. The above considerations correlate with surface tension of polymers, increasing in the same order and with their dielectric constant. Considerable contribution of contact resistance can be also seen from the shift of percolation threshold v^* by 0.12–0.15

with decreasing particle size from 13 to 0.1 μm, which is characteristic of segregated composites, and simultaneous decrease of $\sigma_{\parallel}$ to 10^{-4} (Ohm·cm)$^{-1}$.

2.2. Electrical Properties of Composites with Carbon Fillers

Two types of composites were investigated in the form of plates or filled fibers. The fillers were natural graphite (NG) EUZ-M and synthetic graphite (SG) GMZ with particle size <40 μm (for plates) or <10–15 μm (for fibers). To investigate the effect of particle size the fibers were also prepared with carbon black P268-E (≈300 Å). CM in the form of plates were prepared with PFC method[4,11,12] or by mechanical mixing, described elsewhere.[7] The fibers were prepared by wet-spinning, using copolymer of PTFE and vinylidene fluoride as a fiber forming polymer (CTFVF).[13]

Mechanical mixtures of polypropylene (PP) and graphite were prepared in a blade mixer, then in a laboratory extruder at 220°C with final pressure molding at 190°C and pressure 15 MPa. CM prepared by PFC method have much higher (several orders of magnitude) σ at the same filling v, the difference increasing with decreasing NG concentration (Figures 6, 7 and 8). Gradual decrease of σ from 10 to 10^{-15} (Ohm·cm)$^{-1}$ occurs for mechanical mixtures with decrease of v from 0.6 to 0.2. When $v \leq 0.2$, conductivity depends on the placement of measuring contacts, showing inhomogeneity of specimens. In composites, prepared by PFC method, the range of gradual decrease of σ is shifted to lower values of v with v^* being about 0.08 which is almost two times lower than percolation threshold for statistical mixtures.

Current-voltage curves for these composites are linear for samples with $v > 0.08$ at temperatures between 300 and 4.2 K and current densities up to 1 A/cm^2. The current is inversely proportional to the distance between the electrodes with current density varying within 2–3 orders of magnitude.

Extrapolation of lgσ to $\lg\sigma|_{v=1}$ gives conductivities of graphite particles: for CM with SG, prepared by PFC method $\sigma = 10^3$ (Ohm·cm)$^{-1}$, the same composites with NG have $\sigma = 10^4$ (Ohm·cm)$^{-1}$. Since the values of G differ within an order of magnitude it is not quite clear why at $v \simeq 0.2$ CM with NG have σ which is 2–3 orders of magnitude higher than those with SG.[14] To clarify the point we measured temperature dependence of σ in the interval 4.2–300 K, magnetoresistance $\Delta\rho/\rho$ in magnetic induction range $B = 0$–4 T at 4.2 K and anisotropy of magnetic permittivity at different v (Figures 9–13). It was found that in CM with NG $\Delta\rho/\rho$ changes sign at $v \simeq 0.4$–0.5, i.e. at this concentration intimate contacts between the particles disappear and current flows through polymer interlayers (Figures 9 and 10).

Figure 11 shows the dependence of $\ln(\sigma/\sigma_{4.2K})$ on temperature at $v < 0.5$. Such dependence is characteristic of hopping conduction following the equation $\sigma = \sigma_0 \exp[-(\varepsilon_a/kT)^{1/4}]$, where ε_a is activation energy of hopping conduction, which decreases with increasing filler content and tends to zero at $v \simeq 0.4$–0.5, i.e. at the same loadings where magnetoresistance changes its sign (Figure 12). Low activation energy $\varepsilon_a \simeq (2\text{–}6)\cdot 10^{-4}$ eV mean short jump distances and, consequently, short distances between the localized states. Temperature dependences of σ are quite different for CM with NG or SG, especially at $v = 0.08$ (Figure 13).

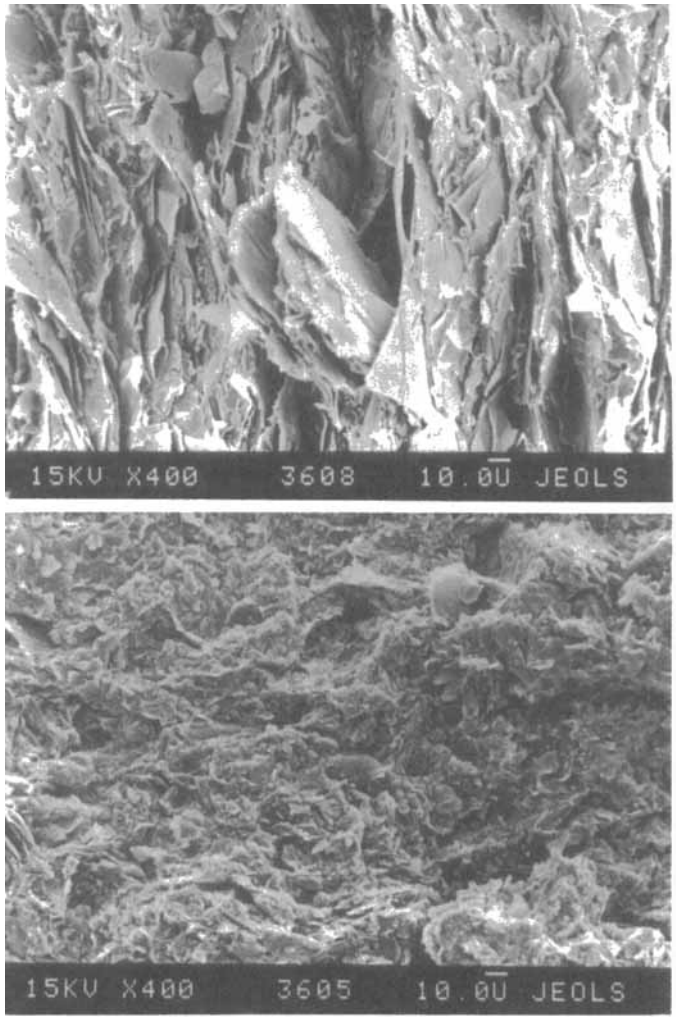

(a)

(b)

FIGURE 6 Microphotographs of fractured surfaces of PP-graphite composites, prepared by PFC method. Composition, wt. %: (1) natural graphite EUZ-M-75, PP-25; and (2) synthetic graphite GMZ-75, PP-25.

This leads to the conclusion that it is the structure of graphite that makes polymer interlayers behave differently in these CM. Indeed, in NG the packets of graphite planes freely contact with polymer, facilitating the injection of current carriers, while the structure of SG is less perfect and the contact of polymer with edge atoms of graphite planes is inhibited (Figure 6). In the latter case injection of current carriers is hindered and conduction of polymer interlayers is by thermally activated carriers of impurity centers. This fact is confirmed by the data on the mobility (μ) of current carriers at 4.2 K. For SG $\mu = 6.4 \cdot 10^2 - 1.4 \cdot 10^3$ cm^2/V·s ($v = 0.3-0.54$), while for NG $\mu = 2 \cdot 10^3 - 4.1 \cdot 10^3$ cm^2/V·s ($v = 0.09-0.62$). In both cases μ depends linearly on v which means that contribution of graphite particles in $\Delta\rho/\rho$ is large, while polymer interlayers share is low.

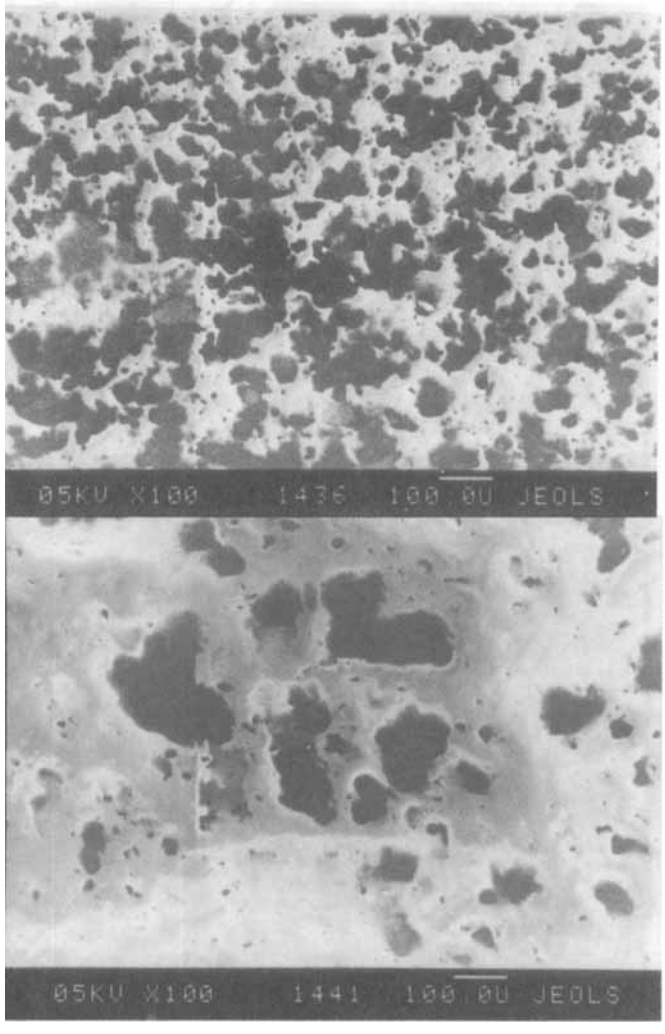

(a)

(b)

FIGURE 7 Microphotographs of the surface of pressure molded films of composites, prepared by: (a) PFC method, PP + natural graphite EUZ-M, v = 9.3 vol. %; and (b) melt mixing, PP + natural graphite EUZ-M, v = 11 vol. %.

Measurements of heat conductivity λ, $\sigma_\perp$ and $\sigma_\parallel$, as well as diamagnetic permittivity show different texture of CM with SG and NG. Conductivity anisotropy $\sigma_\parallel/\sigma_\perp$ = 12–19 for NG and 7 for SG at volume fraction 0.12–0.49 and 0.18–0.49, correspondingly.

Composites with SG have $\lambda_\parallel$ 2–6 W/m·K and $\lambda_\perp$ = 0.8–3 W/m·K for volume fractions 0.09–0.38. Diamagnetic permittivity data show orientation parameter $\overline{\sin^2\theta}$ to be 0.43 for NG, 0.57 for SG, the value for isotropic samples being $\overline{\sin^2\theta}$ = 0.67. This means that in composites with NG graphite planes are oriented mainly parallel to the sample plane, resulting in $\sigma_\parallel > \sigma_\perp$. These results are similar to the data on anisotropy of CM with Al particles, which become anisotropic at certain value of electric field E^* with $\sigma_\perp > \sigma_\parallel$.

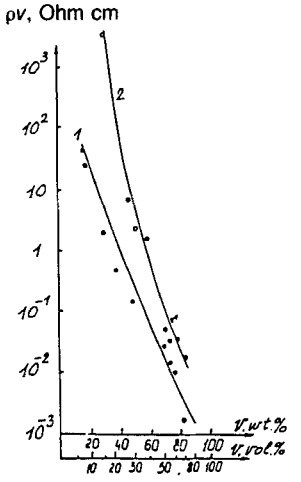

FIGURE 8 Dependence of resistivity $\rho_{\parallel}$ of PP composites, prepared by PFC method on filler concentration: (1) natural graphite EUZ-M; (2) synthetic graphite GMZ. ○ - fraction <40 μm; ● - fraction 40 ÷ 60 μm.

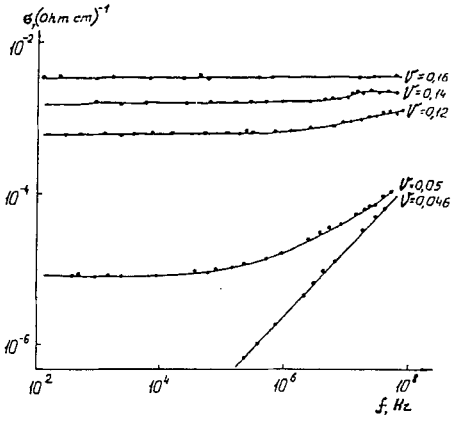

FIGURE 8a Frequency dependence of conductivity for PFC (PP-graphite) with different volume fraction of natural graphite.

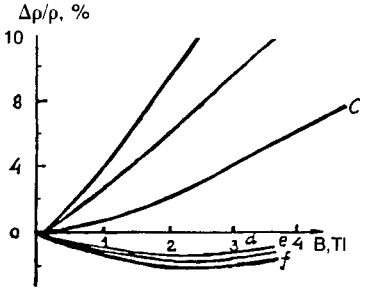

FIGURE 9 Magnetoresistance as a function of magnetic field induction at 4.2 K for composites with SG at different filler vol. fractions: (a) 0.72; (b) 0.62; (c) 0.51; (d) 0.38; (e) 0.31; and (f) 0.27.

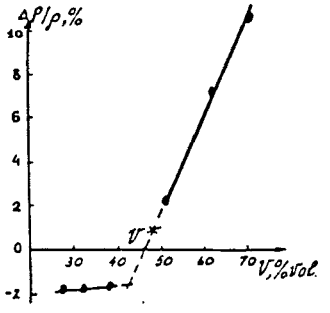

FIGURE 10 Magnetoresistance as a function of graphite vol. fraction for PFC with SG. Magnetic field B = 2.3 T, temperature 4.2 K.

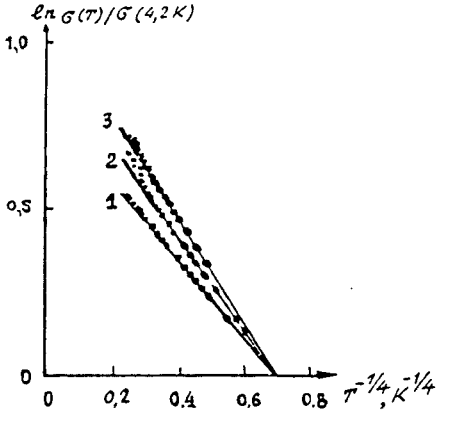

FIGURE 11 Plot of $\ln(\sigma/\sigma_{4.2K})$ versus $T^{-1/4}$ for PFC with SG. Filler volume fraction: (1) 0.38; (2) 0.31; and (3) 0.27.

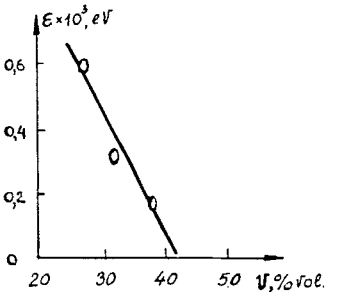

FIGURE 12 Activation energy ε of hopping conduction as a function of graphite content v for PFC with SG.

Composite materials with graphite fillers were also compounded in extruder in four different regimes[7] (Figures 14 and 15). One of the reasons for these investigations was to make homogeneous materials with linear R-l characteristics, i.e. the resistance R being proportional to the length l of the sample. The mixtures were prepared from NG and polymer powders with initial particle size 100–300 μm: polypropylene (PP), low-density polyethylene (LDPE), polyvinylchloride (PVC)

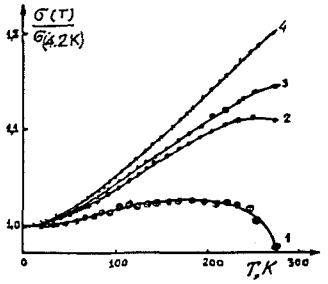

FIGURE 13 Temperature dependence of conductivity for PFC with NG at different volume fraction of graphite; (1) 0.08; (2) 0.20; (3) 0.50; and (4) 0.62.

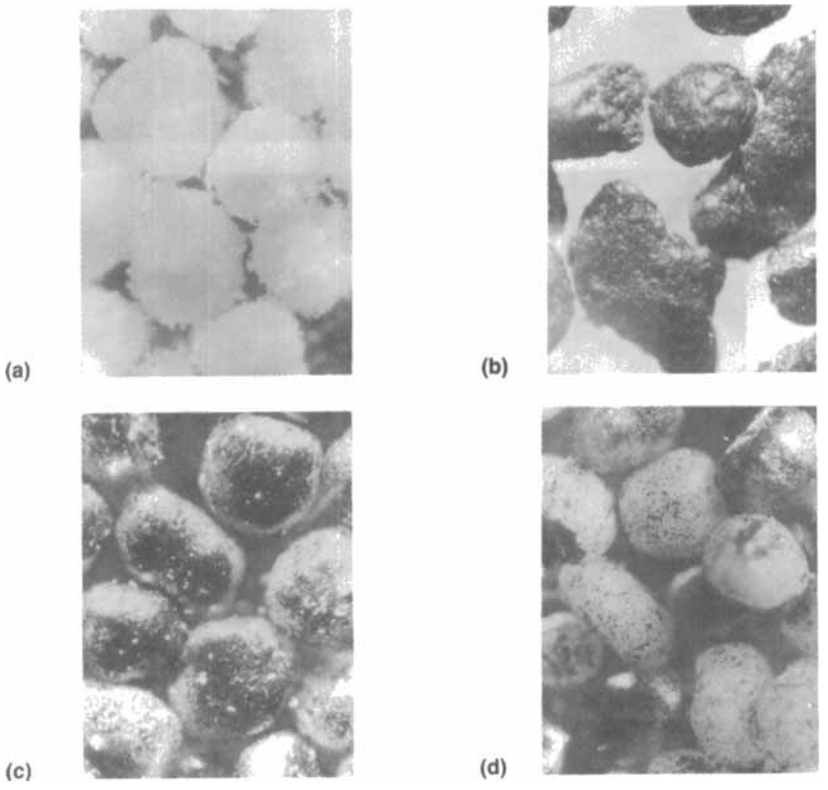

FIGURE 14 Microphotographs of PP particles. (a) initial particles; (b) compounding with natural graphite EUZ-M (80:20) by elastic deformation pulverization; (c) compounding with synthetic graphite GMZ (70:30) by "cold" extrusion; and (d) compounding with synthetic graphite GMZ (60:40) by "cold" extrusion.

and polymethylmetacrylate (PMMA). Conductivity $\sigma_{\|}$ of pressure molded plates was found to depend on the polymer used and extruder regime (Table I).

Mixing in the melt (MM) of NG and PP gives conducting composites ($\sigma_{\|} = 0.2$ $(\text{Ohm}\cdot\text{cm})^{-1}$) only at $\simeq$30 vol. %, while at lower concentrations $\sigma_{\|} < 10^{-12}$ $(\text{Ohm}\cdot\text{cm})^{-1}$. In elastic pulverization regime (EP) conductivity ranged from 1 to 10^{-12} $(\text{Ohm}\cdot\text{cm})^{-1}$, depending on concentration and the type of polymer. Composites prepared by "cold" extrusion (CE) had higher conductivities: $\sigma = 2\text{–}1\cdot10^{-5}$

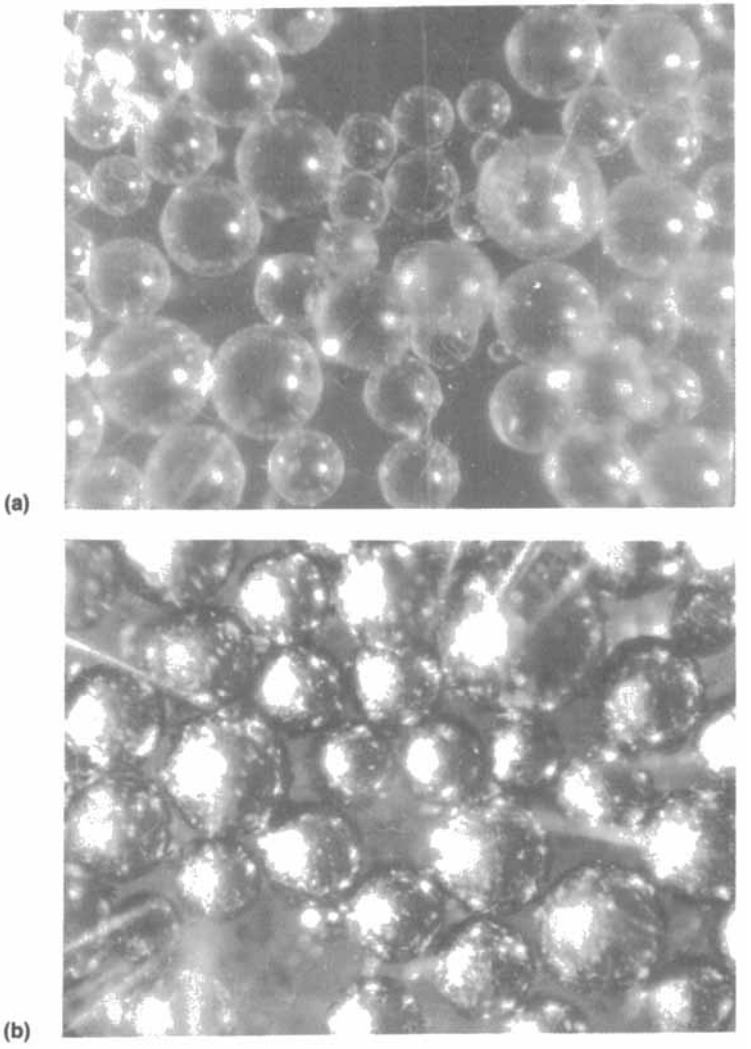

FIGURE 15 Microphotographs of polymethyl metacrylate particles (×400): (a) initial particles, size 200–315 μm; (b) compounding with natural graphite EUZ-M (80:20) by "cold" extrusion.

$(\text{Ohm}\cdot\text{cm})^{-1}$ in the same range of concentrations, $v = 0.09–0.3$. For "dry" mixing (DM) $\sigma = 14.2$ (PP, $v = 0.12$); $\sigma = 7.7$ (PMMA, $v = 0.09$); $\sigma = 0.12$ (PVC, $v = 0.09$) and $\sigma = 5\cdot10^{-2}$ $(\text{Ohm}\cdot\text{cm})^{-1}$ (LDPE, $v = 0.09$). Percolation thresholds were the following: $v^* = 0.1–0.17$, characteristic of statistical mixtures, for MM regime; $v^* = 0.07–0.1$ for EP regime (PP, PVC, PMMA). The lowest threshold values were found in CE and DM regimes: $v^* = 0.05$. R-I characteristics were found to be linear for composites prepared in EP regime, and, as mentioned earlier, for PFC method.

For three-component materials (PP, LDPE, NG), prepared in EP and MM regimes, the addition of only 10 wt. % of PP leads to a sharp increase of σ to 10^{-5} $(\text{Ohm}\cdot\text{cm})^{-1}$ at $v = 0.22$.

TABLE I

Resistivity of CM thermoplast-graphite (Ohm·cm)

Polymer	Filling, wt.%	Melt	Pulverization	"Cold" regime	"Dry" mix
PP	20	$>10^{12}$	840	5	--
	25	$>10^{12}$	--	1.6	0.07
	30	--	38	17.5	--
	50	4.7	4.1	1.8	--
LDPE	20	$>10^{12}$	$>10^{12}$	$8 \cdot 10^{4}$	16.8
	30	--	$>10^{12}$	--	--
	40	--	$3.2 \cdot 10^{6}$	--	--
	50	--	14.8	--	--
PVC	20	$>10^{12}$	1.0	1.1	8.0
PMMA	20	$>10^{12}$	--	0.5	0.13

Formation of fibrous CM with electrophysical and other properties has its special features, related with polymer and filler compatibility, limiting filler particles dimensions, their distribution in the matrix and drawing (Δl).[13] The account of these factors allowed to find optimized compositions for spinning conducting fibers (d = 80 μm), as well as spinning conditions. GMZ graphite and P268-E carbon black concentrations were varied from 0.3 to 0.6; v^* for CM with graphite was $v^* = 0.5$ and for CM with carbon black $v^* = 0.2$. Comparison with films of the same compositions and thickness 200–300 μm shows that in this case $v^* = 0.2$ (carbon black) and $v^* = 0.3$ (graphite). At graphite content $v = 0.49$ and drawing ratio $\Delta l = 80\%$ $\sigma = 1.5 \cdot 10^{-2}$ (Ohm·cm)$^{-1}$, increasing Δl to 87.5% decreases σ to $6.3 \cdot 10^{-3}$ (Ohm·cm)$^{-1}$.

2.3. Electrodynamic Properties of CM with Disperse Particles Fillers

Besides *dc* properties of CM, discussed above, they were also measured in *ac* electromagnetic fields. This allowed to ascertain v^* and structure and find $\sigma(\omega)$, $\varepsilon(\omega)$ and $\mu(\omega)$ at high and microwave frequencies.

In general, for single-phase polymers $\sigma(\omega)$ decreases with frequency, if conductance is thermally activated. The presence of filler makes $\sigma(\omega)$, depending on v, behave differently at concentrations below, above or at the percolation threshold. At low v, when conducting filler particles are isolated and polymer phase is continuous, distinction of $\sigma(\omega)$ is negligible at low frequencies and $\sigma \simeq \sigma(\omega)$. With increasing frequency conductivity also increases, especially in the region close to v^*, when an infinite cluster of conducting particles first develops. At higher concentrations, $v >> v^*$, conducting chains appear in the system, with conductance becoming metallic and $\sigma(\omega)$ may be independent of frequency. Frequency dependence of composites dielectric constant ε_c' is also related to v. In many cases (at $v < v^*$) $\varepsilon_c' \simeq \varepsilon_p'$ (ε_p' is polymer dielectric constant). With increasing v ε_c' increases first gradually and then sharply in the region $v \simeq v^*$. Increase of ε_c' near v^*, according to the effective medium model is due to the increase of capacitance of the system with decreasing interparticle distance. At $v >> v^*$, when continuous chains with metal-like conductance appear, ε_c' decreases. The amplitude of ε_c' at the threshold v^* depends on frequency, decreasing with ω.

Alumoplastics, prepared by PFC method, exhibit continuous increase of ε_c' in the range $v = 0.06$–0.77 (measured at 1 kc/s, without performing in the field)

from 3.3 to 84, $\sigma(\omega)$ being weakly dependent on v. The behavior is different at higher frequency: at 4.8 GHz ε_c' increases from $\simeq 3$ to 60 and σ—from to $\simeq 2 \cdot 10^{-3}$ $(\text{Ohm} \cdot \text{cm})^{-1}$ (at $v = v^* = 0.72$). Fitting of $\sigma(\omega)$ and ε_c' data at 10.5 GHz gives $\sigma(\omega) = 2.7 \cdot 10^{-3}$ $(0.91 - v)^{-2.7}$, showing that v^* in the sample molding plane equals 0.92. Performing in electric field decreases percolation threshold in the field direction from 0.92 to 0.45, these composites being typical matrix systems before the field was applied.

Dynamic electrical properties of CM with carbon fillers prepared by PFC method are distinctly different. For CM with NG ($\omega = 37$ Mc/s) at $v \leq v^* \simeq 0.08$ ε_c' is close to ε_p'. With increasing v ε_c' increases first gradually and then more sharply at $v \simeq v^*$, reaching at $v > v^*$ the value $\simeq 40$ ($v = 0.095$). In the same concentration range $\sigma(\omega)$ increases from 10^{-6} to 10^{-3} $(\text{Ohm} \cdot \text{cm})^{-1}$, but more gradually than *dc* conductivity. Measurements of $\sigma(\omega)$ and ε_c' in the range $\omega = 1-100$ Mc/s show that even around $v^* \simeq 0.08$ $\sigma(\omega)$ is independent of frequency and ε_c' decreases from 100 to 30. This means that in CM with NG intimate contacts between the filler particles appear at low filler concentrations, which was already reported earlier (Figure 8a).

For fibrous composites both $\sigma(\omega)$ and ε_c' increase with increasing concentration of SG and carbon black ($\omega = 4.8$ GHz). There is evidence that distinction between σ of fibers and films of the same composition decreases. Both $\sigma(\omega)$ and ε_c' decrease with increasing Δl: at 80% $\sigma(\omega) = 11 \cdot 10^{-2}$ $(\text{Ohm} \cdot \text{cm})^{-1}$, $\varepsilon_c' = 180$; with Δl changing to 82, 84, 86 and 87.5% the values of $\sigma(\omega)$ and ε_c' are equal, correspondingly, to $8.1 \cdot 10^{-2}$ and 83; $6.3 \cdot 10^{-2}$ and 65; $5.6 \cdot 10^{-2}$ and 56; $4.9 \cdot 10^{-2}$ and 50.

TABLE II

Electrical properties of fibers and films with isotropic fine-grained graphite

Filler concn. % wt.	Drawing ratio %	Time of treatment min	Conductivity *dc* $\text{Ohm}^{-1}\text{cm}^{-1}$	Conductivity *ac* $\text{Ohm}^{-1}\text{cm}^{-1}$	Dielectric constant real part	Dielectric constant imaginary part
			fibers			
30	80	-	$<10^{-9}$	$3.9\ 10^{-4}$	3.4	0.15
50	80	-	10^{-9}	$4.8\ 10^{-3}$	19	1.8
70	80	-	0.019	0.11	135	40
70	80	10	0.18	0.59	290	220
70	80	15	0.42	0.77	180	290
70	82	-	0.012	0.081	83	40
70	84	-	$9.5\ 10^{-3}$	0.063	65	31
70	86	-	$8.2\ 10^{-3}$	0.056	56	24
70	87.5	-	$6.3\ 10^{-3}$	0.049	50	18
			films			
30	-	-	$2.6\ 10^{-3}$	$3.8\ 10^{-3}$	12	1.7
70	-	-	0.26	0.29	135	130
70	-	10	0.35	0.38	217	133
70	-	15	0.42	0.55	145	190

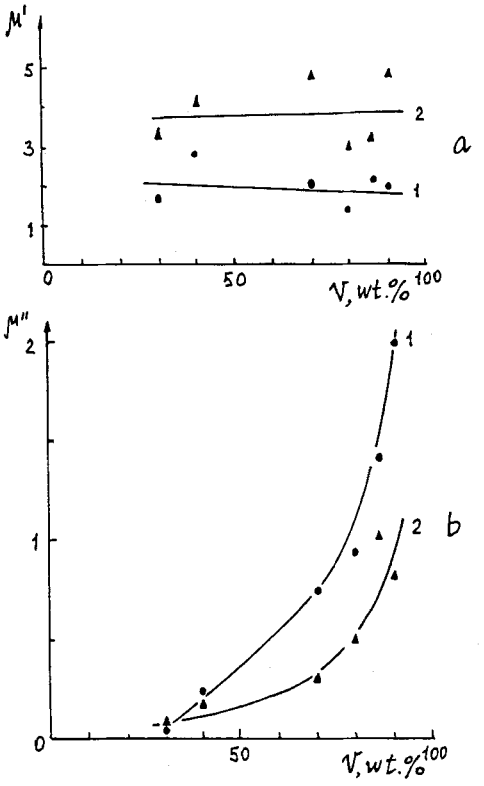

FIGURE 16 Dependence of real μ′ (a) and imaginary μ″ (b) parts of magnetic permittivity of PTFE composite on ferrite concentration, frequency 4.8 GHz, (1) fibers and (2) films.

These changes seem to be due to the increase of interparticle distances, equivalent to decrease of filler concentration (Table II).

Comparison of electrodynamic properties of conducting fibers and fibers filled with Z-type hexaferrite (particle size about 3 μm) gives following results (Figures 16 and 17, Table III). *DC* conductivity $\sigma < 10^{-12}$–10^{-14} $(\text{Ohm}\cdot\text{cm})^{-1}$. Real and imaginary parts of dielectric (ε', ε'') and magnetic (μ', μ'') permittivities were measured in the frequency range 2–12 GHz (Table II). Both for fibers and films μ' is independent of ferrite concentration in the interval $v = 0.14$–0.77, while μ'' gradually increases, reaching maximum value at $v = 0.77$. For fibers $\mu'' = 2.2$ ($\omega = 4.8$ GHz) with density 4.2 g/cm^3. The fibers are mechanically stable with tensile strength 5.8–6.4 MPa. Comparison of the values μ' and μ'' for fibers, compacted isotropic ferrite and textured composite samples (texturization degree 80%) shows that they are higher for fibers, the reason being, probably, orientation of ferrite particles during fiber spinning.

The above investigations demonstrate a definite progress in materials research of disperse particles filled composites, increasing the possibilities of their practical applications.

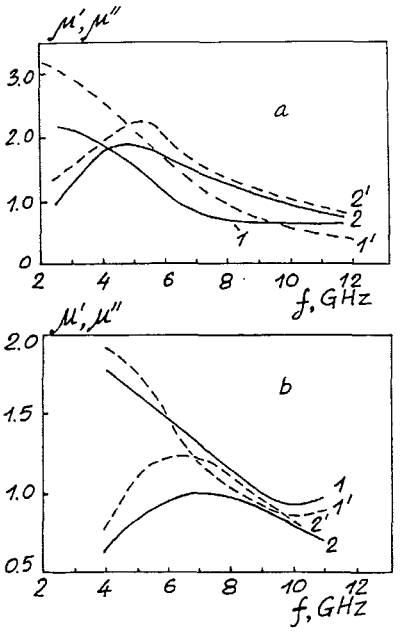

FIGURE 17 Spectra of magnetic permittivity and losses of ferrite-containing materials: 1,1' – μ'; 2,2'' – μ''. a: solid lines—compacted ferrite powder; dotted line—fibers from PTFE and ferrite (77 vol. %). b: samples of epoxy—ferrite (37 vol. %) composites; solid lines—isotropic sample, dotted line—textured sample.

3. COEFFICIENTS OF REALIZATION OF ANISOMETRIC FILLERS CONDUCTIVITY IN COMPOSITE MATERIALS

Previous chapters treated CM with disperse fillers having particle aspect ratio $L/D \simeq 1$ (L, D are effective length and diameter of particles). For CM with fillers having $L/D \neq 1$ v^*, as a rule, is considerably lower, variation of σ and $\sigma(\omega)$ with increasing v being dependent on filler conductivity and interparticle contact resistance R_c. Using different technological methods (PFC, electrochemical polymerization, heat treatment, deposition of conducting or insulating layers) allows to change v^* and prepare conducting or dielectric materials with specific *dc* and *ac* characteristics (σ, $\sigma(\omega)$, ε', ε'', μ', μ'').

Recently in electrophysics of CM, similar to mechanical properties, a concept of coefficient of filler realization (K_r) is increasingly used.[17] This coefficient is useful for investigation of CM with long or short fibers, since all their electrical parameters can be measured before compounding with polymer.

Carbon fiber composites (CFC) with phenol-formaldehyde resin matrix were prepared with Uglen (PAN-based) or UVK (hydrated cellulose-based) carbon fibers having different heat treatment temperatures (HTT) in the range 750–2200°C. Fiber length was varied from 10 to 30 mm, with $L/D \geq 100$. Prepregs were pressure molded to sample size 120 × 15 × 10 mm at 160°C and 32–35 MPa, fiber loading $v = 0.5$. Conductivity σ was measured in the direction of sample length (σ_1), width (σ_2) and thickness (σ_3), the results showing preferred orientation of fibers in the molding plane.[15,16]

TABLE III

Some mechanical and electrodynamic properties of ferrite-filled composite fibers and films of PTFE copolymer. Frequency 4.8 GHz

Material	Ferrite concn. % wt.	Ferrite concn. % vl	Stabilizer	Density g/cm³ measured	Density g/cm³ calculated*	Tensile strgth MPa	Dielectric constant real ε′	Dielectric constant imaginary ε″	Magnetic permittivity real μ′	Magnetic permittivity imaginary μ″
fiber	30	14	polymer	2.25	2.35	-	3.5	0.27	-	0.035
film	"	"	"	2.13	"	-	-	-	-	0.054
fiber	40	20	"	2.4	2.55	15.0	5.0	0.45	1.22	0.26
film	"	"	"	2.3	"	-	-	-	-	0.16
fiber	70	46	"	3.38	3.41	9.1	3.1	0.11	1.80	0.96
film	"	"	"	2.75	"	-	-	-	-	0.39
film	75	52	"	-	3.63	-	-	-	1.83	1.29
fiber	80	59	no stabil.	-	3.86	6.1	-	-	-	-
"	"	"	proxanol	-	"	5.4	-	-	-	-
"	"	"	HSL136-41	-	"	5.8	-	-	-	-
"	"	"	polymer	3.75	"	6.4	5.4	0.20	1.95	1.98
film	"	"	"	3.86	"	-	-	-	-	0.93
fiber	86	69	"	4.07	4.19	4.0	7.0	0.20	2.02	1.87
film	"	"	"	4.3	"	-	-	-	-	1.02
fiber	90	77	"	4.16	4.43	3.0	8.0	0.25	2.11	2.16
film	"	"	"	4.7	"	-	-	-	-	0.93

* - Perrite density was taken 5.2 g/cm³ and copolymer density 1.9 g/cm³.

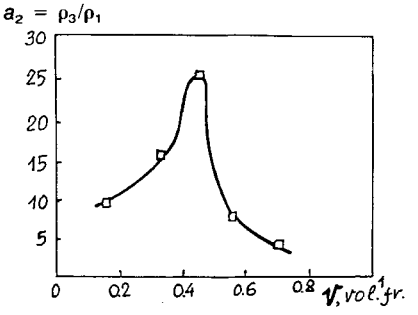

FIGURE 18 Anisotropy a_2 of conductivity of the plastic based on Uglen fibers with HTT 900°C versus fiber volume fraction.

Coefficient of realization of filler conductivity can be defined as $K_r = \sigma/(v \cdot \sigma_f)$ (σ_f is filler conductivity) and may vary from 0 to 1, $K_r = 1$ being the case of complete realization, for example, in unidirectional CFC in σ_1 direction; $K_r = 0$, for example, in matrix CM or when interfiber contacts are specially blocked by surface treatment of fibers.

With HTT of Uglen fibers increasing from 750 to 900°C σ_f increases from 13.5 to 62.5 and σ_1 from 6.2 to 19.2 $(\text{Ohm} \cdot \text{cm})^{-1}$ (Tables IV and V). The value of K_r remains at the level of 0.85–0.88 up to HTT = 770°C, then decreases to 0.55–0.57 with increasing HTT to 800–900°C and corresponding increase of σ_f. Similar behavior is observed for UVK fibers: $\sigma_f = 45.5$, $\sigma_1 = 23.3$, $K_r = 1.1$ (1200°C);

TABLE IV

Dependence of Uglen fibers conductivity (σ_f), conductivity (σ_c) and coefficient of realization (K_r) of phenolic plastics from these fibers on fiber HTT, (v_f = 0.54)

HTT°C	750	760	770	800	880	900
σ_f,1/(Ohm·m)	13.5	17.9	20	31.2	58.8	62.5
σ_c,1/(Ohm·cm)	6.2	8.2	9.6	12.2	17.5	19.2
K_r	0.85	0.85	0.88	0.72	0.55	0.57

TABLE V

Dependence of UVK fibers conductivity (σ_f), conductivity (σ_c) and coefficient of realization (K_r) of phenolic plastics from these fibers on fiber HTT. (v_f = 0.54)

HTT°C	1200	1400	1600	1800	2000	2200
σ_f,1/(Ohm·cm)	45.5	188.7	233	238	270	313
σ_c,1/(Ohm·cm)	26.3	62.5	71.4	76.9	83.3	83.8
K_r	1.1	0.61	0.57	0.60	0.57	0.49

σ_f = 238, σ_1 = 77, K_r = 0.6 (1800°C); σ_f = 313, σ_1 = 84, K_r = 0.5 (2200°C). Decrease of K_r with increasing HTT of fibers can be understood from a simple model: at high σ_f contribution of R_c in overall conductivity is large. With decreasing σ_f fiber resistance becomes comparable to R_c and principal contribution is from the fiber conductivity σ_f, leading to increase of K_r. The value of R_c for these types of fibers and polymer matrix was estimated to be $\simeq 10^4$ Ohm, influencing the values σ_1, σ_2 and σ_3 with changing L/D and HTT of fibers.

It was found, that coefficients of anisotropy $a_1 = \rho_2/\rho_3$, $a_2 = \rho_3/\rho_1$ and $a_3 = \rho_2/\rho_1$ depend on fiber concentration in a different fashion. Their orientation at $v \simeq 0.5$ can be described as packing in the apex angle of a cone with axis oriented along the sample length and elliptical base, the orientation caused by dense packing of fibers during pressure molding. It was an important finding that coefficient a_2 passes a maximum with increasing v: a_2 = 10 at v = 0.2; a_2 = 25 at v = 0.4; a_2 = 5 at v = 0.6 (Figure 18). This can mean that at low concentration interaction between the fibers is weak with minimum degree of orientation, with v increasing to $\simeq$0.4 fibers tend to orient in the molding plane. At $v > 0.4$ further orientation of fibers is hardly possible, instead, interfiber distance is decreased, resulting in decrease of a_2.

In conclusion, electrical properties of short fiber CM in different directions should be taken into account in selecting filler properties and processing CM.

4. CONTROL OF CONDUCTIVITY ANISOTROPY IN COMPOSITES WITH CARBON FABRIC FILLERS

There is extensive literature data on the methods of formation and mechanical properties of glass-, organic- and carbon fiber reinforced plastics with fillers in the

form of fabric.[17,18] From the scattered data it follows that these CM are electrically anisotropic at least in two directions: the value of longitudinal conductivity σ_1 may be larger than σ_2 in the thickness direction, while σ_3 (in the width direction) may equal σ_1 or differ from it to either side, depending on the type of weave; at the same time the difference between σ_1 and σ_2 may be negligible.

Electrical properties of carbon fibers, felts and fabrics have many common features, since they are largely determined by HTT of these fillers. As already was mentioned, they have high anisotropy of conductivity, that can reach in CM $\sigma_1 = 10^1-10^3$ (Ohm·cm)$^{-1}$ with coefficient of anisotropy $a_2 = \rho_3/\rho_1 \simeq 100$ or more. The problem of reducing anisotropy is solved, as it is known, in carbon-carbon CM, when polymer matrix is subjected to HTT, reducing contact resistance, resulting in $a_2 \simeq 2-5$.[19,20] The same result may be attained by using three-dimensional fabrics, ensuring electrical contacts between the layers with conducting "crosslinks."[21] In this case it is necessary to know σ of these "crosslinks," their density depending on σ_1 and possible range of control of anisotropy in CM.

In some cases there is a necessity in hybrid carbon fiber CM with alternating layers, having different values of σ. According to the rule of mixture, the values of $\rho_\parallel$ and $\rho_\perp$ are:

$$\rho_\parallel = (v\sigma_k^\parallel + (1 - v)\sigma_y^\parallel)^{-1}$$

$$\rho_\perp = v\rho_k^\perp + (1 - v)\rho_y^\perp,$$

where $\sigma_k^\parallel$ and $\sigma_y^\parallel$ are longitudinal conductivities of each layer, $\rho_k^\perp$ and $\rho_y^\perp$ are transverse resistivities of the same layers, $\rho_\parallel$ and $\rho_\perp$ are longitudinal and transverse resistivities of hybrid CM.

We investigated several hybrid CM with following lay-up sequence:

1. 17 layers CF_1 + 1 layer CF_2 + 17 layers CF_1;
2. 5 layers CF_1 + (1 layer CF_2 + 5 layers CF_1);
3. 1 layer CF_1 + (1 layer CF_2 + 1 layer CF_1) 17;
4. 5 layers CF_2 + (1 layer CF_1 + 5 layers CF_2) 5,

where CF_1 and CF_2 are different types of carbon fabrics.

Measurements of these CM shows that predicted $\rho_\parallel^T$ and experimental values of longitudinal resistivities are in good agreement, while for $\rho_\perp$ and $a_2 = \rho_\parallel/\rho_\perp$ the coincidence is poor. For sequences 1–4 predicted values $\rho_\parallel^T$ are $1.7\ 10^{-1}$; $3.3\ 10^{-2}$; 10^{-2}; $5.7\ 10^{-3}$; and experimental—$1.82\ 10^{-1}$; $3.45\ 10^{-2}$; $9.81\ 10^{-3}$; $5.28\ 10^{-3}$ Ohm·cm. At the same time, for sequences 1 and 4, for example, $\rho_\perp^T = 136$, $\rho_\perp^e = 70$ and $\rho_\perp^T = 20.6$, $\rho_\perp^e = 6.6$, correspondingly. Predicted and experimental values of a_2 for sequence 1 are $a_2^T = 800$, $a_2^e = 385$ and for sequence 4 – $a_2^T = 13600$, $a_2^e = 1225$. These results show, that it is possible to vary $\rho_\parallel$ in a sufficiently wide range, at the same time changing transverse resistivity.

In order to investigate the effectiveness of using conducting "crosslinks," inserted perpendicular to the molding plane, they were studied both theoretically and experimentally. Figure 19 presents calculated (curve 1) and experimental (curve 2) dependences of $a_2 = \rho_3/\rho_1$ on S_c/S_{cm} (S_c and S_{cm} are the areas of "crosslinks" and

However, it does not mean a complete functionalization of the polymer surface at all, as the high advancing contact angles and the great hysteresis indicate.

The state of complete modification is reached only at a treatment time of about 450 seconds and it is characterized by a total surface free energy of the polymer of about 58 mJ/m^2 as calculated from both the advancing as well as the receding contact angles (Table II). The increase of the total surface free energy from 31 mJ/m^2 for the untreated sample is mainly caused by an increase of the acid-base interactions and only to a minor extent by an increase of the Lifshitz-van der Waals interactions. It is worth noting, that the polymer surface acts as an electron donor as well as an electron acceptor.

From Figures 1 and 2 it must be concluded, that even in the case of the nitrogen plasma the functionalization of the polymer surface is mainly determined by oxygen traces in the plasma deriving from impurities of the nitrogen gas, from oxygen adsorbed by the sample and at the reactor walls, and from leakages in the vacuum system.

The influence of oxygen residues during plasma treatment with inert gases is documented in the literature.[1] However, the fact, that the nitrogen plasma under the specific experimental conditions used in the present work behaves rather like an oxygen plasma contaminated by nitrogen, was unexpected, but may be understood in terms of the classical kinetic theory of gas. According to this theory the number of gas molecules z striking a unit area per second is given by[5]

$$Z = \frac{N_A}{\sqrt{2\pi R 10^{-3}}} \frac{p}{\sqrt{TM}} \tag{4}$$

where N_A is Avogadro's number, R the gas constant, p the pressure, T the absolute temperature, and M the molecular weight of the gas.

Using Equation (4) the collision rate of oxygen molecules deriving from air leakages at a basic pressure of 2 Pa, as it was realized in our dc plasma reactor,

TABLE II

Surface free energy and its components in terms of Equations (1) and (2) of plasma treated PE (calculated from advancing contact angle values)

treatment	γ_l^{tot}, mJ/m^2	γ_l^{LW}, mJ/m^2	γ_l^+ mJ/m^2	γ_l^- mJ/m^2
untreated	32.5	32.4	0.002	0.03
nitrogen, rf	60.6	41.6	3.26	27.5
nitrogen, dc	57.9	41.3	2.21	31.1
oxygen, rf	55.2	40.4	2.35	23.5
oxygen, dc	53.5	40.3	1.57	27.9
hydrogen, rf	34.9	34.5	0.06	0.9
hydrogen, dc	34.5	34.4	0.01	0.2

The properties of carbon CM, especially with natural and synthetic graphite fillers are also important. For example, CM with NG, prepared by PFC method have high strain sensitivity $K = \Delta R/(R \cdot \varepsilon)$, where R is initial resistance before stretching (Figure 21). In these CM the dependence of K on v passes a maximum. At $v < v^*$ $K = 2.0$, at $v = v^*$ K reaches a peak value of 100–150 and at $v > v^*$ K decreases: $K = 37$, 20 and 10 at $v = 0.03$, 0.08 and 0.21, respectively, reducing to $\simeq 0$ at $v > 0.5$. For CM, prepared by mechanical mixing the peak value of K is $\simeq 50$ at $v = v^*$, reducing to 5 at larger loadings ($v = 0.09$–0.3). The values of K found at $v = v^*$ are more than an order of magnitude higher than those for common wire strain-gauge resistors. As can be seen from Figure 21, at $\varepsilon \leq 10^{-2}$ in loading-unloading cycle $R(\varepsilon)$ coincide for loading and unloading (curve 3), while at $\varepsilon > 10^{-2}$ hysteresis caused by plasticity of matrix is observed, with loop width increasing at lower and higher v. Hysteresis is reduced by lowering temperature 20–50°C, while strain sensitivity remains high. At $\varepsilon \geq 10^{-2}$ relaxation phenomena is observed, with partial decrease of R ($\simeq 10\%$), the reason being orientation of filler particles. After removing deformation, conductivity recovers, relaxation time reducing with the increase of T.

Heat conductivity of CM (Figure 20) in the molding plane is substantially higher

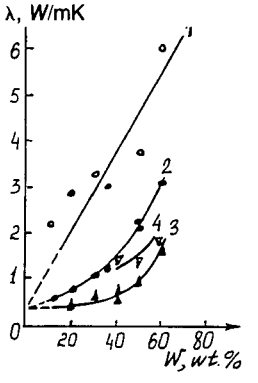

FIGURE 20 Dependence of heat conductivity of composites in the molding plane (1,4) and in transverse direction (2,3) on graphite concentration: 1,2-synthetic graphite; 3,4-natural graphite.

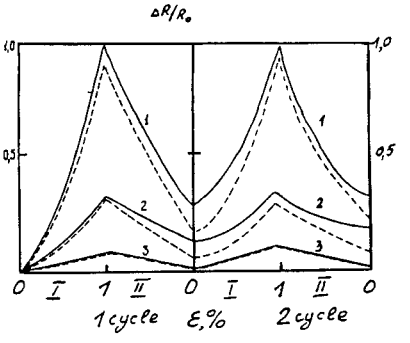

FIGURE 21 Change of relative longitudinal resistance $\Delta R/R_0$ versus ε in two cycles (loading-unloading) for CM with natural graphite, prepared by PFC method; solid lines = 300 K, dotted lines = 250 K. Graphite volume fraction v: (1) 0.04; (2) 0.08; and (3) 0.21.

for SG filler (curve 1) compared to NG. For comparison, mechanical mixtures of PP and NG have $\lambda_\perp = 0.9$ W/m·K at $v = 0.21$, while for PFC composites $\lambda_\perp = 1.1$ W/m·K at $v = 0.15$. Like electrical conductivity, heat conductivity of CM is anisotropic, with $\lambda_\parallel/\lambda_\perp = 3$.

The above properties of CM allow to use them as heat conducting elements or strain gauges. Other distinctive features of CM with graphite, prepared by PFC method, are: compared to mechanical mixtures, 7–8 orders of magnitude greater value of $\sigma_\parallel$ at $v = 0.1$; weak dependence of σ on frequency with relatively high

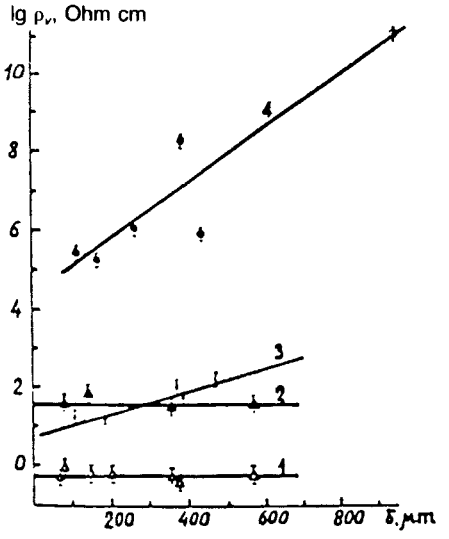

FIGURE 22 Resistivity of PFC (1,2) and mechanically mixed (3,4) composites versus specimen thickness. Graphite concentration: 1,3-25; 2,4-10.5 vol. %.

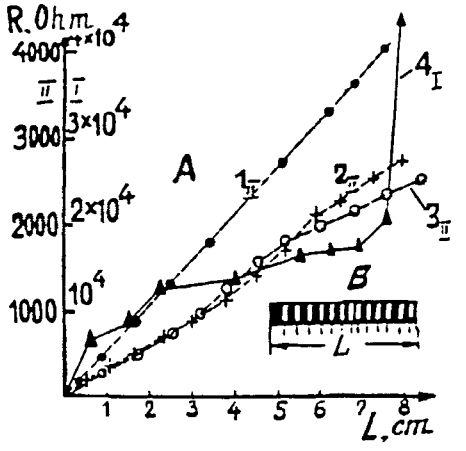

FIGURE 23 A. R-l characteristics of composites from natural graphite EUZ-M, PP (1,2,4) or PE (3), prepared by PFC method (1) or mechanical mixing (2–4). Graphite concentration, vol. %: (1) 9; (2) 33; (3) 10; and (4) 18. B. Arrangement of electrodes on a specimen. Resistivity of composites Ohm·cm: (1) 32 ± 2; (2) 5.2 ÷ 9.2; (3) 10.2 ÷ 25.5; and (4) 80 ÷ 1200.

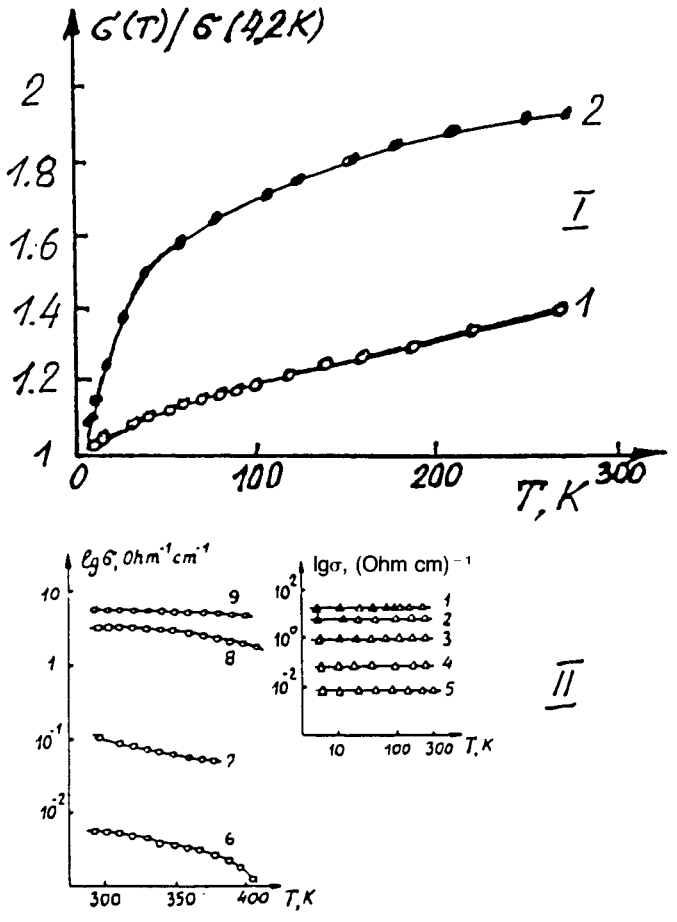

FIGURE 24 I. Dependence of relative conductivity of composites on temperature. PFC composite of PP and synthetic graphite GMZ: (1) 62; (2) 31 vol. %. II. Temperature dependence of conductivity for PFC composites of PP and natural graphite. Graphite concentration, vol. %: (1) 61; (2) 40; (3) 35; (4) 10; (5) 8; (6) 10.5; (7) 25; (8) 33.

ε′; linearity of current-voltage characteristics up to 1A/cm^2; high homogeneity of properties (Figures 22 and 23) with linear *R-L* characteristics and independence of σ on specimen thickness; unusual magnetic properties; resistance to external shocks, such as multiple heating-cooling cycles from helium to room temperature; low temperature coefficient of resistance ($\approx 10^{-4}$ K^{-1} for CM with NG in temperature range 4.2–300 K, Figure 24). Mechanical properties of PFC CM are also unusual. Young's modulus increases 5-fold with increasing v from 0 to 0.38 (for mechanical mixtures modulus is 1.6 times lower). Elongation at break decreases to ≈10% at $v = 0.05$. Tensile and compression strength are practically constant up to $v = 0.49$, while mechanical mixtures become brittle already at $v = 0.043$.[22]

Such materials are prospective for use in corona-discharge or precipitation filters (Figure 25) and low-temperature heaters.

Fibers with carbon or ferrite fillers may probably be used in shielding or scattering materials. The increasing saturation of the environment with electromagnetic fields

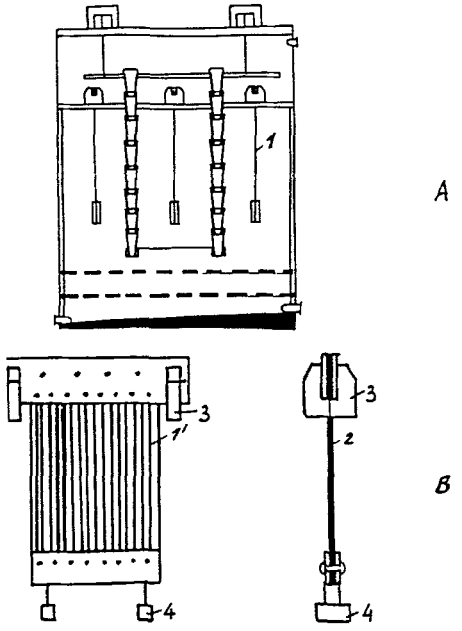

FIGURE 25 General view of a filter (A) with electrodes from conducting composite: · precipitation electrode; — detailed view of precipitation electrode (front view); · design of precipitation electrode, side view (B); · girder; 4 - load.

of various frequencies and power lead to increasing interference of electronic devices and may be harmful to man, in USA, as well as in Russia. That was the reason, why US Federal Communications Commission (FCC) issued in 1983 standard FCC N20780, which limits levels of electromagnetic fields of different frequencies in industrial and domestic environment. Consumption of CM for shielding is limited for economic reasons (only 500 tons in 1986), since, for example, conducting paints are much cheaper, although sometimes not as effective.

Composites with carbon fibers are prospective as conductors with high mechanical properties, their conductivity being considerably higher compared to particle filled CM. Recently a tendency is observed towards using them as acid batteries leads or in electronics.

The use of conducting fabrics, as well as carbon fibers is limited by economic reasons. The experience in their production and use, as well as new world situation give hope for their increased use as electrodes, contact elements of electrical machines (collectors, contact rings of low-power machines) or as imitations of rocks for geological modelling (i.e., model composites, that are electrically adequate to coal, mineral or oil-rich rocks).

6. CONCLUSION

Electrophysical materials science is an extensive field of research, vital both scientifically and technologically. Its target is development of new methods for pro-

ducing CM, investigation of their electrodynamic properties and on these grounds creation of basis for practical realization of results.

Acknowledgment

The author wishes to express his sincere thanks to the following persons of ISPM staff: Ph.D. V. G. Shevchenko, researchers I. A. Tchmutin, S. V. Letyagin, A. V. Buts, Ph.D. N. G. Ryvkina, researcher E. A. Trushina and to colleagues of other institutes. Special thanks are to Prof. N. S. Enikolopyan for continuous cooperation and support of this research field.

References

1. Carbon Black-Polymer Composites: The Physics of Electrically Conducting Composites/ed. E. K. Sichel. N.Y., Basel: Marcell Dekker, 1982, 212 pp.
2. C. Klason and J. Kubat, *J. Appl. Pol. Sci.*, **24**, 831 (1975).
3. Yu. I. Vasilenok, Prevention of Static Electrization in Polymers. (in Russian) L., Khimiya, 1981, 208 pp.
4. USSR Patent N1240761, CO8F 292/00; CO8L 23/12; CO8K 3/04; HO1B 1/24. Conducting Material and the Method for Making the Same.
5. P. G. Filippov, V. G. Shevchenko, A. T. Ponomarenko, V. A. Benderskiy and A. A. Ovchinnikov, Electrical Properties of Polymer Composites with Conducting Disperse and Fibrous Fillers. (in Russian). Review Information, NIITEKHIM, N1 (219), 1984, M., 53 pp.
6. V. G. Shevchenko and A. T. Ponomarenko, Transport Processes in Conducting Particle-Filled Composites. *Adv. Chem. (USSR)*, **52**, 1336–1349 (1983).
7. V. G. Shevchenko, A. Yu. Karmilov, O. V. Demicheva, A. T. Ponomarenko and N. S. Enikolopyan. New Conducting Polymer Composites: Outlook and Applications. In: Mechanical Modellings of New Electromagnetic Materials (Proceedings of the IUTAM Symposium, 2–6 April, 1990, Stockholm, Sweden), R. K. T. Hsieh, Ed. Elsevier, Amsterdam, 1990, pp. 197–201.
8. Yu. V. Borisov, V. G. Grinnev, O. I. Kudinova, L. A. Novokshonova, A. T. Ponomarenko, N. G. Ryvkina, V. G. Shevchenko, G. M. Tarasova and I. A. Tchmutin. Electrical Properties of Polyolefine-Based Alumoplastics. // *Acta Polymerica*, **43**, 131 (1992).
9. Yu. V. Borisov, V. G. Grinev, O. I. Kudinova, L. A. Novokshonova, A. T. Ponomarenko, G. M. Tarasova, I. A. Tchmutin and V. G. Shevchenko. Composite Materials Based on Polyolefines and Aluminum Powder with Thermal Conductivity and Dielectrical Properties. / Proceedings of the 3rd Japan-USSR Joint Symposium on Advanced Composite Materials. Moscow, USSR, September 30–October 6, 1991, p. 230 (1993).
10. A. Malliaris and D. T. Turner, *J. Appl. Phys.*, **112**, 614 (1971).
11. F. S. Dyachkovskiy and L. A. Novokshonova, *Adv. Chem. (USSR)*, **53**, 200–222 (1984).
12. A. T. Ponomarenko, V. G. Shevchenko and N. S. Enikolopyan. Formation Processes and Properties of Conducting Polymer Composites. *Adv. Pol. Sci.*, **96**, 125–147 (1990).
13. E. A. Trushina, I. A. Tchmutin, L. A. Koreshkova, S. S. Schukin, V. G. Shevchenko, A. T. Ponomarenko and Yu. G. Kryazhev. Preparation and Electrical Properties of Composite Fibers from PTFE Copolymer and Carbon Fillers. *Khim. Volokna*, **3**, 48 (1992).
14. A. S. Kotosonov, S. V. Kuvshinnikov, I. A. Tchmutin, V. G. Shevchenko, A. T. Ponomarenko and N. S. Enikolopyan. Anisotropic Properties and Mechanism of Conduction in Graphite-Filled Polypropylene. *Vysokomol. Soed.*, **33**, pp. 1746–1752.
15. S. V. Letyagin, E. V. Goncharova, R. L. Mokienko, V. G. Shevchenko, O. I. Mikhailova, E. P. Kucher and A. T. Ponomarenko. Electrical Properties of Composites, Undirectionally Reinforced with Short Carbon Fibers. Proceedings of MICC-90, Elsevier, 1991, pp. 757–761.
16. S. V. Letyagin, V. G. Shevchenko, E. V. Goncharova, E. P. Kucher, R. L. Mokienko, A. T. Ponomarenko and N. S. Enikolopyan. Coefficient of Realization of Filler Conductivity in Composite Materials. // *Acta Polymerica*, **43**, 62 (1992).
17. Carbon Fibers and their Composites. E. Fitzer (Ed.). Springer N.Y., Berlin, 1985.
18. Handbook of Composite Materials. G. Lubin (Ed.) Van Nostrand Reinhold, N.Y., 1982.

19. V. S. Ostrovskiy, Yu. S. Virgilyev, V. I. Kostikov and N. N. Shapkov, Synthetic Graphite. (in Russian). M., Metallurgiya, 1986, 272 pp.
20. A. S. Fialkov, Carbon Materials. (in Russian), M., Energiya, 1979, 319 pp.
21. Yu. M. Tarnopolskiy, *Mekh. Polimerov*, **3**, 541–542 (1972).
22. N. M. Galashina and A. T. Ponomarenko, *et al.*, Abstracts of IUPAC Macro-83, Bucharest, Romania, Sept. 5–9, 1983, Sect. 6–7, p. 121.